Stabilisation of individual generators with SVC designed via phase plane partitioning

AUTHOR(S):

Zhou, J.

CITATION:

Zhou, J.. Stabilisation of individual generators with SVC designed via phase plane partitioning. IET Control Theory & Applications 2010, 4(4): 601-612

ISSUE DATE:

2010

URL:

http://hdl.handle.net/2433/128926

Stabilization of Individual Generators with SVC Designed via Phase Plane Partitioning

Jun Zhou*

Abstract

By phase plane partitioning, dynamics of individual generators in multimachine systems are approximately represented by means of a sequence of linear time-invariant (LTI) state-space equations, based on which various static VAR compensators (SVC) are designed to stabilize the individual generators by exploiting the well-known LTI stabilization techniques. More precisely, we work out state feedback controlled SVCs through pole assignment and least quadratic regulation, respectively. The suggested SVCs can also accommodate transient and steady-state performance specification on the generator's dynamics, besides stabilization. Numeric examples clearly illustrate efficacy and convenience of the stabilization techniques.

Key words: swing equation, stabilization, pole assignment, least quadratic regulation, static var compensator, piecewise linearization

1 Introduction

Stabilization of synchronous generators is a key issue [2] in power systems, to which numerous papers have been devoted by working on the so-called conventional (or simplified, classical) swing equations [10]. Recent results can be found in [1, 24, 25, 26].

Robustly stabilizing individual generators in a complicated multimachine network in the Lyapunov stability sense via state feedback controlled flexible ac transmission system (FACTS) [11, 12] is considered in the study. Stabilization of individual generators in large-scale multimachine systems is absolutely indispensable and of more practical significance than the techniques aiming at stabilizing all generators [1, 2, 3, 4] simultaneously but at the price of complex control and communication devices and relatively high cost, even though some of these control techniques are claimed to be implementable in such and such local and decentralized fashions [5, 6, 7, 8, 9].

In the former part of the paper, swing equations for individual generators are derived while modeling uncertainties inside generators and perturbation from the outside multimachine network are treated as disturbances. Then a piecewise linearization approach [17, 32], which implies phase plane partitioning, is adopted for approximating the swing equations. Equipped with the piecewisely linearized swing equations, we work out SVCs for stabilizing individual generators in the latter part, using pole assignment (PA) and least quadratic regulation (LQR), respectively. The stabilization algorithms possess many advantages, and can cope with damping windings and disturbances, and eventually result in robust stabilization. The SVCs can also accommodate transient

*Dept. of Electrical Engineering, Kyoto University, Kyotodaigaku-Katsura, Nishikyo-ku, Kyoto 615-8510, Japan. Tel: +81-75-3832260, zhouj@kuee.kyoto-u.ac.jp

and steady-state performances on generators. In contrast, by the so-called equal area criterion technique [10, 11, 15], neither damping windings nor disturbances can be dealt with accurately. Lyapunov methods are also frequently employed for stabilizing generators, which usually involve nonlinear control and are generally of high conservatism [13, 16, 14].

Outline. Section 2 describes the swing equations for individual generators with SVCs and its piecewise linearization. Section 3 talks about stabilization via SVCs using PA and LQR techniques. Illustrative examples are sketched in Section 4. Section 5 collects remarks.

2 Individual Swing Equation and its Piecewise Linearization

2.1 Swing Equations in Multimachine Networks and Reduction

As is well known [2, 26], the swing equation system for modeling the generator dynamics in a multimachine power system with n genertors under the assumptions of constant rotor winding flux, constant mechanical torque, and the absence of voltage regulators can be given by

$$\begin{cases} \dot{\delta}_i = \omega_i \\ \dot{\omega}_i = -D_i J_i^{-1}\omega_i + M_i^{-1}P_i \\ \qquad\quad - \sum_{k=1}^{n} b_{ik} J_i^{-1} \sin(\delta_i - \delta_k - \theta_{ik}) \end{cases} \tag{1}$$

where the subscript $i = 1, 2, \cdots, n$ means the ith generator. D_i: damping of amortisseur windings; P_i: constant mechanical power input minus local load; δ_i: torgue angle of the ith machine with respect to the center of axis; ω_i: rotor anglar velocity with respect to the system angular frequency ω_s; J_i: inertia constant and $M_i = J_i\omega_s$; θ_{ik}: complement of transfer admittance phase between internal nodes i abd k; b_{ik}: maximal real power transferred between internal nodes i and k.

Without losing generality, let us concentrate attention on the swing equation (1) for the 1st generator. If we view all δ_i $(i \neq 1)$ as disturbances to δ_1, then

$$\begin{aligned} & \sum_{k=1}^{n} b_{1k} J_1^{-1} \sin(\delta_i - \delta_k - \theta_{ik}) \\ = \; & \sum_{k=1}^{n} b_{1k} J_1^{-1} (\sin\delta_1 + \Delta\delta_1) \\ =: \; & b_1 M_1^{-1} \sin\delta_1 + M_1^{-1} P_\Delta \end{aligned} \tag{2}$$

where $|\Delta\delta_1| \leq 1$, $b_1 = \sum_k \omega_s b_{1k}$ and P_Δ is a power term to equivalently representing power swings caused by other interconnected generators. Using (2) back to (1), we obtain

$$\begin{cases} \dot{\delta}_1 = \omega_1 \\ \dot{\omega}_1 = -D_1 J_1^{-1}\omega_1 + M_1^{-1}(P_1 + P_\Delta) - b_1 M_1^{-1} \sin\delta_1 \end{cases}$$

Comparing the differential equation with the so-call swing equation for single machine infinite bus (SMIB) power systems [2, 10, 29], we see that an individual generator in a multimachine system can be modeled as an SMIB system with influence from other generators being treated as disturbance to the mechanical input power. This is the starting point of the individual generator stabilization idea. The next section gives detailed explanation about such a re-modeling approach.

2.2 Equivalent Swing Equation for an Individual Generator

An individual generator system (IGS) in Figure 1 is isolated locally from its multimachine network, where $\overline{\text{IGS}}$ represents the multimachine portion connected with the IGS via a transmission line

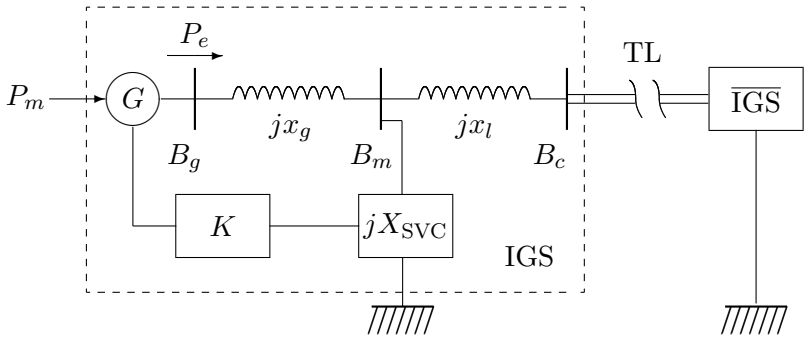

Figure 1: Configuration of the IGS in multimachine networks

(TL). B_g, B_m and B_c, respectively, are the generator internal bus, an intermediate bus to which a shunt SVC is connected, and a local bus connected to TL. x_g is the reactance between B_m and B_g, while x_l is that between B_m and B_c. The SVC is viewed as variable susceptance X_{SVC} as in [10, 11]. P_m is the mechanical power to the generator from turbine and governor, and P_e is the electrical power viewed at B_g. K represents a feedback control to the SVC.

Based on some results of [10] and the re-modeling technique suggested in the previous section, an equivalent swing equation for the dynamics of the generator rotor with a shunt SVC being implemented as in Figure 1 can be given by

$$\Sigma: \quad \begin{cases} \dot{\delta} = \omega \\ \dot{\omega} = -\dfrac{D}{J}\omega - \dfrac{b\sin\delta}{xM} + \dfrac{P_m + P_\Delta}{M} \end{cases} \tag{3}$$

where

$$b = E_c E_g, \quad x = x_g + x_l - X_{\mathrm{SVC}} x_g x_l$$

In the above, E_c and E_g are the virtual voltages of the buses B_c and B_g, respectively, which are introduced for computing the electric output power P_e. Voltage deviations between the real voltages of B_c and B_g and the virtual ones, E_c and E_g, are taken into account as power perturbation P_Δ. Complicated but weak dynamics of the shunt SVC can also be viewed as model uncertainties and added to P_Δ. In this sense, Eq. (3) can be validated generally for describing the swing dynamics of an individual generator in a multimachine background.

δ and ω, respectively, are the generator rotor angular displacement and velocity with respect to a reference axis on B_c rotating at ω_s [19], where ω_s is the system angular frequency.

J: combined moment of inertia in the generator rotor (kg·m^2); and $M = J\omega_s$.

D: mechanical and electrical dampings due to amortisseur windings [18, p. 35],[27, p. 145], which depends on ω by the winding design [27, p. 145].

P_Δ: modeling error and power disturbance measured at the generator rotor. Generally, it is hard to handle P_Δ rigorously. We assume P_Δ is a bounded disturbance.

To facilitate our statements, let δ be the output of the IGS, that is, $y = \delta$. Conventionally, δ is also called the power angle of the generator, which determines the generation efficiency of the generator in the IGS. In short, the IGS is described by the state-space representation

$$\Sigma: \quad \begin{cases} \dot{\zeta} = A\zeta + B_1(\delta)x^{-1} + B_2(P_m + P_\Delta) \\ y = C\zeta \end{cases} \tag{4}$$

which is also called the swing equation for lack of better words and

$$\begin{cases} \zeta = \begin{bmatrix} \delta \\ \omega \end{bmatrix}, \quad A = \begin{bmatrix} 0 & 1 \\ 0 & -D/J \end{bmatrix} \\ B_1(\delta) = \begin{bmatrix} 0 \\ -b\sin\delta/M \end{bmatrix}, \quad B_2 = \begin{bmatrix} 0 \\ 1/M \end{bmatrix} \\ C = \begin{bmatrix} 1 & 0 \end{bmatrix} \end{cases}$$

Carefully examining (4), one will realize that it is essentially nonlinear. Our first question is: is it possible to transform (4) into LTI ones so that the well developed LTI techniques can be utilized for stabilizing the IGS? By constructing piecewisely linearized approximate expressions for (4), we show in the subsequent discussion that this idea does work.

2.3 Piecewisely Linearized Swing Equations and Features

Firstly, we partition the phase plane of the swing equation (4) as described in Figure 2. In Figure 2,

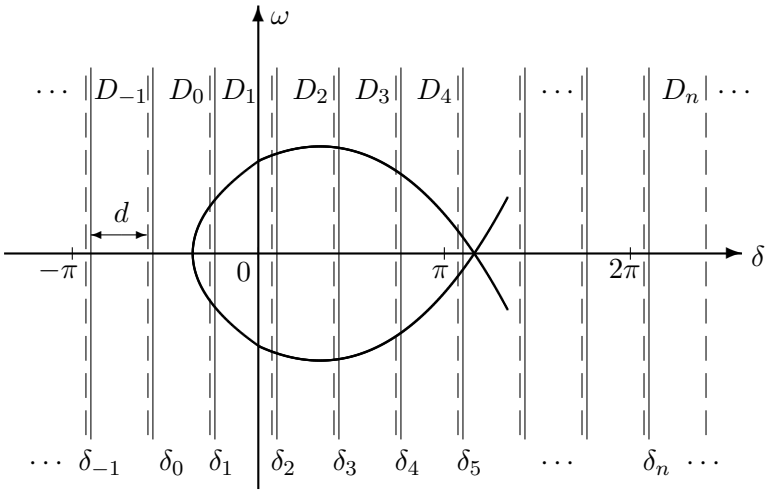

Figure 2: Phase plane partitioning for piecewise linearization

the subscript n indicates the sub-regions; and the solid lines are the left (included) boundaries for $\{D_i\}$ while the dashed lines stand for their right (non-included) boundaries. We assume that the sub-regions $\{D_i\}$ are sufficiently many such that

$$\cup_i D_i = \cup_i \{(\delta, \omega) \ : \ \delta_i \le \delta < \delta_{i+1}\}$$

contains all phase portraits of (4) that interest us, while each sub-region D_i is narrow, namely d is sufficiently small, such that $\delta \doteq \delta_i$ is reasonable for every $\delta \in D_i$.

Secondly, based on the sub-region sequence $\{D_i\}$, we define the following piecewisely linearized state-space representation Σ_i for (4) whenever $\delta \in D_i$.

$$\Sigma_i : \quad \begin{cases} \dot{\zeta}_i = A\zeta_i + B_1(\delta_i)x^{-1} + B_2(P_m + P_\Delta) \\ y = C\zeta_i \end{cases} \tag{5}$$

where ζ_i is the state vector of Σ_i; or an alternative for ζ over $\delta \in D_i$. Clearly, A, B_2 and C are the same as to those in (4), but $B_1(\delta_i)$ becomes constant for each fixed i and given by

$$B_1(\delta_i) = \begin{bmatrix} 0 \\ -b\sin\delta_i/M \end{bmatrix} =: \begin{bmatrix} 0 \\ -\Theta_i \end{bmatrix}$$

where Θ_i is obviously defined. Clearly, (5) is LTI, and thus the piecewise linearization forms a group of LTI state-space representations for the swing equation (4) according to $\{D_i\}$.

Thirdly, we consider dynamic and structural features of Σ_i. Now we can claim that

$$\lim_{t\to t_0^+} ||\zeta(t) - \zeta_i(t)|| = 0 \tag{6}$$

and $\zeta(t), \zeta_i(t) \in D_i$ for any initial vectors $\zeta(t_0) = \zeta_i(t_0) \in D_i$. Here $t \to t_0^+$ means t tends to the initial time t_0 from its right. Indeed, it is evident that

$$\begin{cases} ||\zeta(t) - \zeta_i(t)|| \le ||\zeta(t) - \zeta(t_0)|| + ||\zeta_i(t) - \zeta_i(t_0)|| \\ \lim_{t\to t_0^+} ||\zeta(t) - \zeta(t_0)|| = 0, \quad \lim_{t\to t_0^+} ||\zeta_i(t) - \zeta_i(t_0)|| = 0 \end{cases}$$

The above limitations follow from continuity of $\zeta(t)$ and $\zeta_i(t)$ with respect to t [20, 29]. The convergence relationship of (6) implies that the dynamics of Σ can be approximated by those of Σ_i as accurately as desired if the sub-region sequence $\{D_i\}$ is fine enough.

Finally, we scrutinize controllability and observability of Σ_i. By definition, the controllability matrix with regard to x^{-1} is

$$Q_{c,i}^{x} = [\, sI - A \,|\, B_1(\delta_i) \,] = \left[\begin{array}{cc|c} s & -1 & 0 \\ 0 & s + D/J & -\Theta_i \end{array}\right]$$

and the controllability matrix with regard to P_m is

$$Q_{c,i}^{P_m} = [\, sI - A \,|\, B_2 \,] = \left[\begin{array}{cc|c} s & -1 & 0 \\ 0 & s + D/J & M^{-1} \end{array}\right]$$

In addition, the observability matrix in term of y is

$$Q_{o,i} = \left[\begin{array}{c} sI - A \\ \hline C \end{array}\right] = \left[\begin{array}{cc} s & -1 \\ 0 & s + D/J \\ \hline 1 & 0 \end{array}\right]$$

Remark 1 *We collect facts about controllability and observability.*

(i). On the one hand, whenever $\sin\delta_i \neq 0$*, it holds that*

$$\operatorname{rank}(Q_{c,i}^{x}) = 2, \quad \forall\, s \in \mathcal{C}$$

Namely, for any Σ_i *in which* $\sin\delta_i \neq 0$*,* $(A, B_i(\delta_i))$ *is controllable by the* PHB *rank criterion. On the other hand, it holds in each* Σ_i *that*

$$\operatorname{rank}(Q_{c,i}^{P_m}) = 2, \quad \operatorname{rank}(Q_{o,i}) = 2, \quad \forall\, s \in \mathcal{C}$$

Namely, (A, B_2) *is always controllable and* (A, C) *is always observable by the* PHB *rank criterion. Controllability of* (A, B_2) *means that state feedback control on* P_m *can stabilize the system, too,*

though it is not practically applicable. Observability of Σ_i *is a key requisite for the* H_2 *and* H_∞ *performance synthesis [30]. To avoid distracting the reader, we will not go further about them.*

(ii). If $\sin\delta_i = 0$, $\mathrm{rank}(Q^x_{c,i}) = 1 < 2$ *at* $s = 0$*; namely, the corresponding system* Σ_i *is not controllable in term of* x^{-1}*. This controllability defectness may cause us trouble for stabilization. Fortunately, however,* $\sin\delta_i = 0$ *can be avoided by selecting* δ_i *as shown in Figure 2. In view of this, it is our standing assumption in the sequel that* $\sin\delta_i \neq 0$ *for any* i*.*

2.4 Feedback Controlled SVC and the Closed-loop IGS

Based on Remark 1, it makes sense to introduce into Σ_i the following state feedback so that closed-loop control performances, say stability, can be improved or secured.

$$x^{-1} = [\, K_{1i} \;\; K_{2i} \,]\zeta_i =: K\zeta_i \tag{7}$$

where K means the feedback control in Figure 1. In practical generators, though ω can be measured directly, δ cannot be measured directly with instruments. Fortunately, from the first differential equation of (3), we see that δ can be retrieved by an integration circuit output with ω being the input, or equivalently adding a PI controller to the measured signal ω. Alternatively, δ can be calculated by numeric integration about ω when computer control is employed. In view of this, it is meaningful to consider stabilization via feedback in terms of δ and ω.

Substituting (7) for (5), the closed-loop state-space representation is

$$\Sigma_{i,c}: \quad \begin{cases} \dot\zeta_i = (A + B_1(\delta_i)[\, K_{1i} \;\; K_{2i} \,])\zeta_i + B_2(P_m + P_\Delta) \\ y = C\zeta_i \end{cases} \tag{8}$$

For our later use, we determine the characteristic polynomial and transfer function for all the closed-loop state-space representations $\Sigma_{i,c}$, which will play a key role in the discussion.

For each i, the characteristic polynomial of $\Sigma_{i,c}$ is

$$\begin{aligned} & |sI - A - B_1(\delta_i)[\, K_{1i} \;\; K_{2i} \,]| \\ = & \begin{vmatrix} s & -1 \\ K_{1i}\Theta_i & s + D/J + K_{2i}\Theta_i \end{vmatrix} \\ = & \; s(s + D/J + K_{2i}\Theta_i) + K_{1i}\Theta_i \\ = & \; s^2 + (D/J + K_{2i}\Theta_i)s + K_{1i}\Theta_i \end{aligned} \tag{9}$$

which implies that the eigenvalues of the state matrix $A + B_1(\delta_i)[\, K_{1i} \;\; K_{2i} \,]$ are

$$p_{1,2} = -\frac{D/J + K_{2i}\Theta_i}{2} \pm \sqrt{\Big(\frac{D/J + K_{2i}\Theta_i}{2}\Big)^2 - K_{1i}\Theta_i} \tag{10}$$

which says that by choosing K_{1i} and K_{2i}, $p_{1,2}$ can possess negative real parts so that the closed-loop system $\Sigma_{i,c}$ is asymptotically stable. In other words, we can design a state feedback controlled SVC, in form of (7), such that $\Sigma_{i,c}$ is stabilized. When the same state feedback controlled SVC is implemented piecewisely in the swing equation (3), then the concerned individual generator is stabilized accordingly due to convergence of (6).

The transfer function between P_m and $y(=\delta)$ in $\Sigma_{i,c}$ is

$$G_{i,c}(s) = C(sI - A - B_1(\delta_i)[\, K_{1i}, \; K_{2i} \,])^{-1}B_2$$

From the specific expressions of C and B_2, we only need to compute the $(1,2)$-term in $\mathrm{adj}(sI - A - B_1(\delta_i)[K_{1i}\ K_{2i}])$, which is nothing but its $(2,1)$-cofactor, that is, $(-1)^{2+1} \times (-1) = 1$. This, together with (9), implies immediately that

$$G_{i,c}(s) = 1/[M(s^2 + s(D/J + K_{2i}\Theta_i) + K_{1i}\Theta_i)] \tag{11}$$

3 Stabilization of Individual Generator Systems with SVC

This is the main context, which introduces various state feedback controlled SVCs so as to stabilize the IGS. The suggested stabilization algorithms are constructed by taking advantages of the piecewisely linearized swing equations, together with the LTI techniques.

Our basic question is: how can we design a feedback controlled SVC, by working on Σ_i, such that the individual generator G in Figure 1 is stabilized?

3.1 Stabilization via Pole Assignment (PA) SVC

In what follows, we are going to explain how stabilization is achieved via state feedback controlled SVCs in form of (7) from a pole assignment point of view.

3.1.1 SVCs Designed through Pole Assignment

To facilitate our statements, assume that λ_1 and λ_2 are the desired poles in $G_{i,c}(s)$ for any i. For the resulting feedback gains K_{1i} and K_{2i} to be meaningful, λ_1 and λ_2 are either a pair of conjugates with negative real parts or two real negative numbers. Needless to say, one can assume different closed-loop poles for each specific $G_{i,c}(s)$ to flexibly reflect our performance requirements on each sub-region D_i. This brings no essential difficulties in the following arguments. We leave the details for the reader. The closed-loop transfer function with λ_1 and λ_2 can be written as

$$G_c(s) = 1/[M(s-\lambda_1)(s-\lambda_2)] = 1/[M(s^2 - (\lambda_1+\lambda_2)s + \lambda_1\lambda_2)]$$

Comparing $G_{i,c}(s)$ in (11) to $G_c(s)$, we are led to

$$\begin{cases} K_{1i}\Theta_i = \lambda_1\lambda_2 \\ D/J + K_{2i}\Theta_i = -(\lambda_1+\lambda_2) \end{cases}$$

which yields that the feedback gains should be

$$\begin{cases} K_{1i} = \Theta_i^{-1}\lambda_1\lambda_2 \\ K_{2i} = -\Theta_i^{-1}(D/J + \lambda_1 + \lambda_2) \end{cases} \tag{12}$$

3.1.2 Transient/Steady-State Specification via PA SVCs

From the following discussion, we will assert that by adjusting K_{1i} and K_{2i}, not only stability but also some transient and steady-state features of the closed-loop IGS can be specified.

(i). We see the closed-loop poles λ_1 and λ_2 can be chosen such that $G_c(s)$ is stable and possesses the desired steady-state output. To see this, let δ_e be the steady-state expectation of δ; namely, the power angle of the generator. We notice that

$$\delta_e = \lim_{t\to\infty}\delta(t) = \lim_{s\to 0} sG_c(s)\frac{1}{s}P_m = \frac{P_m}{M\lambda_1\lambda_2}$$

where P_m is a step signal. It follows that λ_1 and λ_2 should be prescribed by

$$\begin{cases} \mathrm{Re}(\lambda_i) < 0, \quad i = 1, 2 \\ \lambda_1 \lambda_2 = \dfrac{P_m}{M\delta_e} \end{cases} \tag{13}$$

Clearly, the first condition of (13) guarantees that $G_c(s)$ is stable, while the second condition leads that $G_c(s)$ has the steady-state output evaluation δ_e. The latter can be interpreted equivalently after comparing $G_{i,c}(s)$ with $G_c(s)$ as that the feedback gain K_{1i} should satisfy

$$K_{1i} = \frac{P_m}{b\delta_e \sin\delta_e} \tag{14}$$

which says that to attain the desired power angle δ_e of the closed-loop IGS, the feedback gain K_{1i} in the SVC should be fixed according to (14).

Furthermore, we examine the steady-state time response of the closed-loop IGS when the feedback gain of (14) is implemented, by working on the closed-loop transfer function $G_{i,c}(s)$ of (11). Again, assuming that P_m is a step signal, we have by the Laplace transform that

$$\begin{aligned} \lim_{t\to\infty} \delta(t) &= \lim_{s\to 0} sG_{i,c}(s)\frac{1}{s}P_m \\ = \quad \frac{P_m}{MK_{1i}\Theta_i} &= \frac{P_m}{M\dfrac{P_m}{b\delta_e \sin\delta_e}\dfrac{b\sin\delta_i}{M}} \\ = \quad \frac{\delta_e \sin\delta_e}{\sin\delta_i} &\to \delta_e \quad (\text{as } \sin\delta_i \to \sin\delta_e) \end{aligned}$$

which says that using the feedback gain K_{1i} given by (14), we can attain the desired power angle δ_e, if the feedback gain K_{2i} is taken such that δ dynamics in (8) can be driven to a neighborhood of δ_e; or if we can fix K_{2i}, together with K_{1i} of (14), such that (8) is stabilized. Fortunately, such K_{2i} always exists since (8) is also controllable and we examine (10) carefully.

(ii). We see that the poles λ_1 and λ_2 can affect the transient behaviour of Based on (13), λ_1 and λ_2 should be assigned either on the half-circle as a pair of conjugate poles, denoted by crosses, or on the negative real axis as two real poles, denoted by double-crosses, as in Figure 3. We note

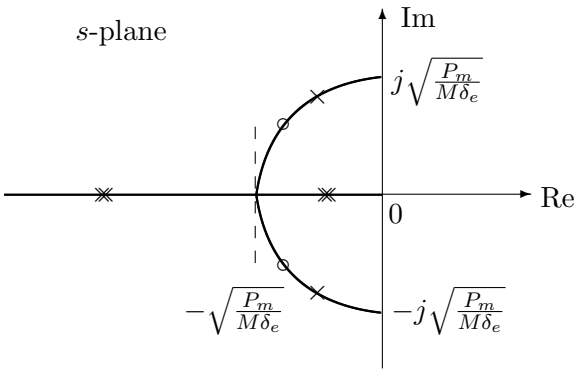

Figure 3: Location of the closed-loop poles λ_1 and λ_2

that λ_1 and λ_2 can be adjusted on the half-circle or the negative real axis such that stability and

the steady-state feature are guaranteed, while some transient features of the closed-loop IGS can be specified at the same time. For example, with conjugate λ_1 and λ_2 locating at the circles of Figure 3, the closed-loop IGS goes to the steady state faster than those locating at the crosses.

3.2 Stabilization via Least Quadratic Regulation (LQR) SVC

In this section, we consider stabilization of the swing equation (3) by implementing SVCs that are determined by means of the least quadratic regulation theory.

3.2.1 SVCs Designed through LQR Technique

More precisely, we formulate the following LQR problem about the piecewise linearized swing equation Σ_i of (5), which will bring us with LQR SVCs that stabilize (3).

$$\min_{x^{-1}} J_i = \int_0^\infty (\zeta_i^T Q_i \zeta_i + x^{-2}\gamma_i) d\tau \tag{15}$$

where the 2×2 weighting matrix $Q_i^T = Q_i$ is positive definite and $\gamma_i > 0$ is a constant. Recalling by Remark 1 that $(A, B_1(\delta_i))$ is a controllable pair, we assert from the LQR theory that the optimal control of (15) in term of x^{-1} is a state feedback given by

$$x^{-1} = -\gamma_i^{-1} B_1^T(\delta_i) P_i \zeta_i =: K\zeta_i \tag{16}$$

where $P_i^T = P_i$ is the unique and positive definite solution to the Riccati algebraic equation

$$P_i A + A^T P_i + Q_i - \gamma_i^{-1} P_i B_1(\delta_i) B_1^T(\delta_i) P_i = 0 \tag{17}$$

Implementing the state feedback (16) to Σ_i, the corresponding closed-loop IGS is

$$\Sigma_{i,c}: \quad \begin{cases} \dot{\zeta}_i = (A - \gamma_i^{-1} B_1(\delta_i) B_1^T(\delta_i) P_i)\zeta_i + B_2(P_m + P_\Delta) \\ y = C\zeta_i \end{cases} \tag{18}$$

which is stable; i.e., $\mathrm{Re}(\lambda((A - \gamma_i^{-1} B_1(\delta_i) B_1^T(\delta_i) P_i)) < 0$. Indeed, we can show this by using the Lyapunov function $V(\zeta_i) = \zeta_i^T P_i \zeta_i$ and (17) and observing its derivative along (18).

3.2.2 Transient/Steady-State Specfication via LQR SVCs

Now let us observe the steady-state features of $\Sigma_{i,c}$ if the feedback gain K is determined via the optimum of (16). To this end, we write

$$Q_i = \begin{bmatrix} q_{11i} & q_{12i} \\ q_{12i} & q_{22i} \end{bmatrix}, \quad P_i = \begin{bmatrix} p_{11i} & p_{12i} \\ p_{12i} & p_{22i} \end{bmatrix}$$

Then trivial deductions about the Riccati algebraic equation (17) yield

$$\begin{cases} q_{11i} - \gamma_i^{-1}\Theta_i^2 p_{12i}^2 = 0 \\ q_{12i} + p_{11i} - (D/J)p_{12i} - \gamma_i^{-1}\Theta_i^2 p_{12i} p_{22i} = 0 \\ q_{22i} + 2(p_{12i} - (D/J)p_{22i}) - \gamma_i^{-1}\Theta_i^2 p_{22i} = 0 \end{cases}$$

whose solution can be explicitly written as follows.

$$\begin{cases} p_{12i} = |\Theta_i|^{-1}\sqrt{q_{11i}\gamma_i} \\ p_{22i} = \dfrac{\sqrt{D^2/J^2 + \gamma_i^{-1}\Theta_i^2(q_{22i} + 2|\Theta_i|^{-1}\sqrt{q_{11i}\gamma_i})} - D/J}{\gamma_i^{-1}\Theta_i^2} \\ p_{11i} = -q_{12i} + (D/J)p_{12i} + \gamma_i^{-1}\Theta_i^2 p_{12i}p_{22i} \end{cases} \tag{19}$$

Furthermore, the transfer function between P_m and $y(=\delta)$ in the corresponding closed-loop IGS, namely $\Sigma_{i,c}$, can be given by

$$\begin{aligned} G_{i,c}(s) &= C(sI - A + \gamma_i^{-1}B_1(\delta_i)B_1(\delta_i)^T P_i)^{-1}B_2 \\ &= 1/[M(s^2 + (D/J + \gamma_i^{-1}\Theta_i^2 p_{22i})s + \gamma_i^{-1}\Theta_i^2 p_{12i})] \end{aligned} \tag{20}$$

Therefore, the steady-state output of $\Sigma_{i,c}$ when P_m is a step signal is

$$\lim_{t\to\infty}\delta(t) = \lim_{s\to 0} sG_{i,c}(s)\frac{1}{s}P_m = \frac{P_m}{|\Theta_i|M}\sqrt{\frac{\gamma_i}{q_{11i}}}$$

Again let the desired power angle be δ_e. Then we conclude that if setting

$$q_{11i} = \frac{\gamma_i P_m^2}{M^2\Theta_i^2\delta_e^2} > 0 \tag{21}$$

and choosing q_{12i} and q_{22i} such that Q_i is positive definite (obviously, such Q_i always exists), then introducing the LQR SVC defined in (16) to the swing equation (3), the closed-loop IGS will be stabilized while the desired power angle δ_e is attained.

3.3 PA and LQR SVCs Subject to Constraints

In practical SVCs, the susceptance $X_{\rm SVC}$ is usually restricted by constraints on their specifications and maintenance costs. In this section, we consider stabilization of the IGS with PA or LQR SVCs under constraints on their susceptance specification given by

$$X_{\min} \le X_{\rm SVC} \le X_{\max} \tag{22}$$

with $X_{\min} < 0$ and $X_{\max} > 0$. In other words, we consider determining the feedback gain K defined in (7) such that the susceptance $X_{\rm SVC}$ of the corresponding feedback controlled SVC satisfies the constraint inequalities (22), while the closed-loop IGS system is stabilized.

To find possible PA and LQR SVCs subject to constraints, we resort to the piecewise control idea again. On the one hand, if $X_{\min} \le X_{\rm SVC} \le X_{\max}$ is true under the pole assignment or least quadratic regulation, then the resulting PA and LQR SVCs are implemented into the IGS as they are; on the other hand, if $X_{\rm SVC} < X_{\min}$ or $X_{\rm SVC} > X_{\max}$ by the pole assignment and least quadratic regulation, then we set the SVC at $X_{\min}$ or $X_{\max}$ as appropriately. In this piecewise control process, stability of the closed-loop IGS when $X_{\min} \le X_{\rm SVC} \le X_{\max}$ is guaranteed by the PA and LQR SVCs. Therefore, if the closed-loop IGS is stable when the SVC is set at $X_{\min}$ or $X_{\max}$, one can assert readily that stabilization of the IGS with SVCs subject to the constraint (22) is completed. Hence, to validate piecewise stabilization of the IGS with SVCs subject to constraints, we must examine stability of the closed-loop IGS when the SVC is set at $X_{\min}$ or $X_{\max}$.

We notice that stability of the closed-loop IGS with the SVC being $X_{\min}$ or $X_{\max}$ must be checked by investigating the swing equation (4), which is nonlinear. Let us consider local stability of the swing equation (4) when $X_{\rm SVC}$ is fixed at $X_{\min}$ or $X_{\max}$. Local stability means dynamic behaviour of the state vector ζ at a small neighborhood around a concerned state-space point. For our purpose, we re-write the first equation of (4) as follows.

$$\dot{\zeta} = A(x,\delta)\zeta + B_2(P_m + P_\Delta)$$

where

$$A(x,\delta) = \begin{bmatrix} 0 & 1 \\ \dfrac{-b\sin(\delta)}{M\delta x} & \dfrac{-D}{J} \end{bmatrix}$$

The characteristic polynomial of $A(x,\delta)$ yields the following eigenvalues:

$$\lambda_{1,2}(A(x,\delta)) = -\frac{D}{2J} \pm \sqrt{\frac{D^2}{4J^2} - \frac{b\sin(\delta)}{M\delta x}} \tag{23}$$

Based on (23), we observe local stability of the closed-loop IGS in terms of δ and x: (i) if $\sin(\delta)/\delta > 0$, both eigenvalues have negative real parts for any $x > 0$; or the closed-loop IGS is locally stable around such δ and for any $x > 0$; (ii) if $\sin(\delta)/\delta < 0$, both eigenvalues have negative real parts for any $x < 0$; or the closed-loop IGS is locally stable around such δ and for any $x < 0$.

Bearing in mind the above facts, we can decide $X_{\rm SVC}$ is to be set at $X_{\min}$ or at $X_{\max}$, depending on $\sin(\delta)/\delta > 0$ and $\sin(\delta)/\delta < 0$ and in term of x (note that $x = x_g + x_l - X_{\rm SVC}x_g x_l$). Apparently, such control laws are not unique and merely sufficient conditions for the closed-loop IGS to be stabilized with SVCs that are set at upper or lower bounds.

3.4 Remarks on Stability Robustness with SVC

Power disturbance P_Δ, stemming from modeling formulation and perturbation of the external multimachine power network $\overline{\rm IGS}$, has been included in the swing equation (3). Now we show concisely robustness of stabilization can be guaranteed. We recall the fact that the farther from the imaginary axis on the left-half complex plane the closed-loop poles of an LTI system are, the stronger the stability robustness is against disturbance, as is known in the control theory.

(i). Stability robustness with PA SVCs. In $\Sigma_{i,c}$ of (8), where an SVC in form of (7) is installed, the desired poles are assigned at λ_1 and λ_2. Hence, to enhance stability robustness is equivalent to having $|{\rm Re}(\lambda_{1,2})|$ as large as possible. In terms of (12), the bigger the feedback gain K_{2i} is, the better; namely, a higher speed feedback is expected for enhancing stability robustness. We note that K_{1i} need to be manipulated for the steady-state characteristics. It is generally not effective to utilize K_{1i} for stability robustness enhancement.

(ii). Stability robustness with LQR SVCs. In $\Sigma_{i,c}$ of (18), where an SVC is installed, it is evident from (20) that the closed-loop poles of $G_{i,c}(s)$ are determined by p_{11i} and p_{22i}. Since p_{11i} is employed for the steady-state specification, we are left with p_{22i} for improving stability robustness. Fortunately, however, this can be simply achieved by larger q_{22i} in the weighting matrix Q_i if we mention the solution formulae in (19). This again infers that a bigger speed feedback gain K_{2i} should be reflected in the measure function J_i.

4 Numeric Illustrations

We show via numeric illustrations that the piecewisely linearized swing equation is an effective representation for the swing equation and that the suggested feedback controlled SVCs in Section 3 can stabilize our example IGS, while some transient and steady-state features of the closed-loop IGS can be specified or improved. Table 1 lists the coefficients of the example IGS.

Table 1: Coefficients of the example individual generator

b:	maximum power capacity	950 (kw)
D:	amortisseur damping constant	95
J:	combined inertia moment	550 (kg·m^2)
ω_s:	system angular frequency	$2\pi \times 60$ (rad/sec)
P_m:	mechanical power	475 (kw)
x_g:	reactance between B_m and B_g	0.6 (Ω)
x_l:	reactance between B_m and B_c	0.4 (Ω)

4.1 Phase Portraits of Swing Equation and its Piecewisely Linearized Ones

Now we plot phase portraits for the swing equation (3) and its piecewisely linearized ones defined by (5). In Figure 4, all the phase portraits are plotted from the same initial conditions for our comparison purpose, and d is the partitioning parameter described in Figure 2.

We see from Figure 4 that when the phase plane is partitioned into $\{D_i\}$ with d being sufficiently small, the phase portraits of the piecewisely linearized swing equations, that is (b), (c) and (d) of Figure 4, have no numerically discernible difference from those of the swing equation (3) given in (a) of Figure 4. This exactly reflects what we have seen in the convergence relationship (6).

4.2 Illustrative Examples with PA and LQR SVCs

Throughout the section, all the time responses are plotted via the second-order Runga-Kutta algorithm [28] with $[\delta(0), \omega(0)]^T$ being randomly given within $\delta(0) \in [-1, 1]$ and $\omega(0) \in [-1, 1]$, and the step size is 0.1(sec). In the following figures, the solid lines represent the rotor angular displacement δ (rad), while the dashed lines stand for its rotor angular displacement velocity ω (rad/sec). The SVC actions are plotted also with solid lines. In each single figure, numeric results for 5 different initial conditions are illustrated for the sake of limited space. The power disturbance P_Δ is assumed to be a white noise of $P_\Delta \in [-20, 20]$ (kw).

(i). Illustrative examples with PA SVCs.

In the cases (b), (c) and (d) of Figure 5, the steady-state power angle is specified at $\delta_e = 72^\circ$ or 1.2566 (rad) by properly choosing the closed-loop poles $\lambda_{1,2}$ as illustrated in (13) based on piecewisely linearized swing equations with $d = 2\pi/10$. Compared to the time responses of the generator without SVC, namely the case (a) of Figure 5, the dynamics of the generator are stabilized with SVCs that are controlled by the state feedback determined through pole assignment. It is worth mentioning that without SVC, the generator may simply run out of synchronism or become unstable, as one can see from (a) of Figure 5.

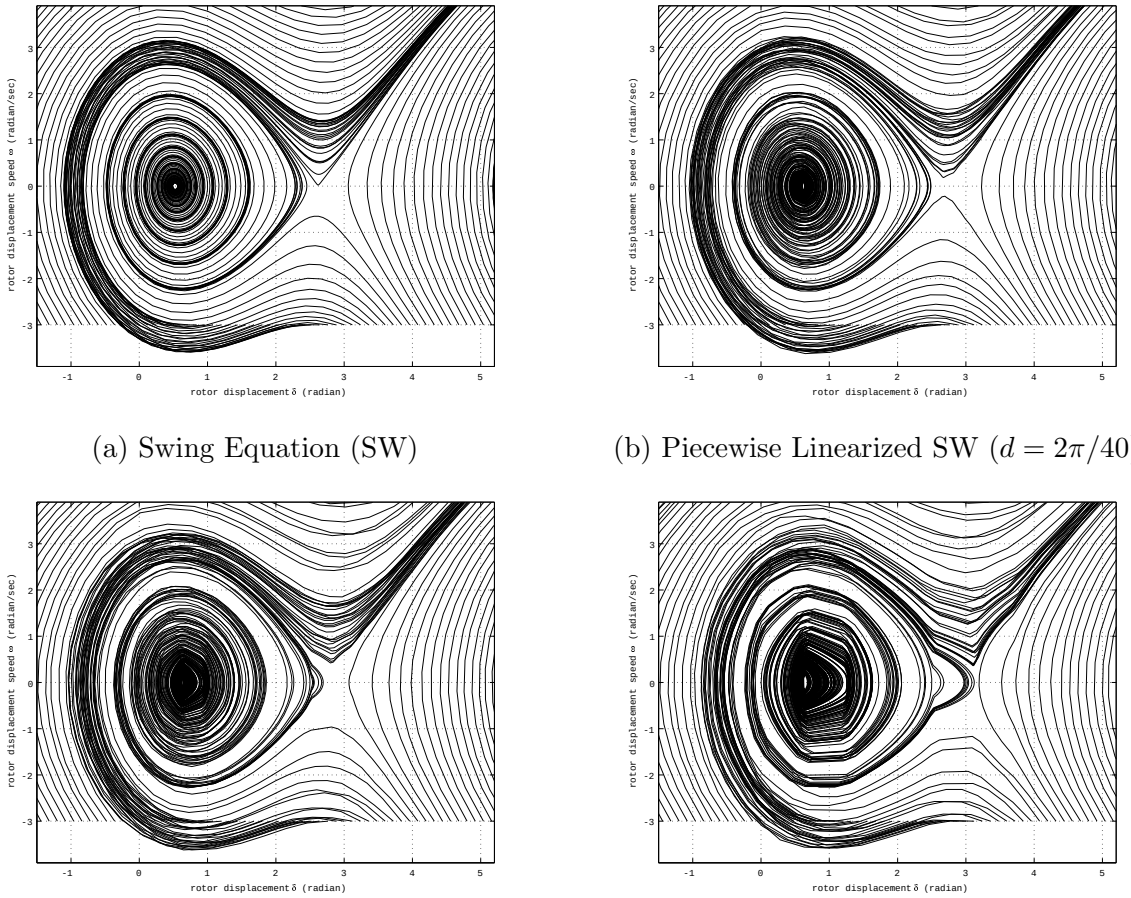

(a) Swing Equation (SW)

(b) Piecewise Linearized SW ($d = 2\pi/40$)

(c) Piecewise Linearized SW ($d = 2\pi/20$)

(d) Piecewise Linearized SW ($d = 2\pi/10$)

Figure 4: Phase portraits of the IGS and its piecewise linearized ones

It is also evident from (b) and (c) in Figure 5 that whenever the closed-loop poles $\lambda_{1,2}$ satisfy (13), some transient features of the time response of the closed-loop IGS can also be modified as well. In our examples, the power angle curve of (b) goes to its steady-state point more quickly than that of (c), due to the real parts specification difference in $\lambda_{1,2}$. Furthermore, if $\lambda_{1,2}$ are chosen to be real, then no overshots appear in the time responses as we can seen from (d) of Figure 5.

It should be pointed out that in the steady states of Figure 5, some bang-bang actions appear in the PA SVCs. Such bang-bang actions are caused by power disturbance P_Δ. Indeed, when the power distubance P_Δ is reduced or simply removed, our numeric simulation reveals bang-bang actions in PA SVCs correspondingly decrease or completely diminish. This is also the case for all the following illustrative examples.

(ii). Illustrative examples with LQR SVCs.

For simplicity, we take $\gamma_i = 1$, $q_{11i} = q_{22i}$ satisfying (21), and $q_{12i} = q_{21i} = 0$ for each i. Clearly, the corresponding weighting matrix Q_i is positive definite. In Figure 6, we observe two cases with $\delta_e = 72^\circ$ and $\delta_e = 60^\circ$, respectively, which say that by choosing q_{11i} appropriately, the steady-state power angle can be specified via LQR SVCs, while the closed-loop IGS is stabilized.

Comparing the curves in Figure 6 with those in Figure 5 (d), we see that impact of LQR SVCs on time responses are similar to that of PA SVCs that assign two real poles. In other words, LQR

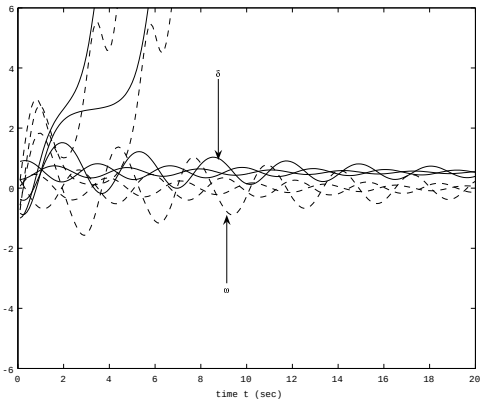

(a) Time responses without SVC

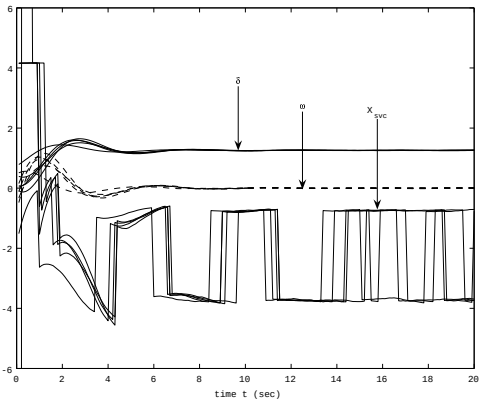

(b) PA SVC with $\lambda_{1,2} = -0.5 \pm 1.2542j$

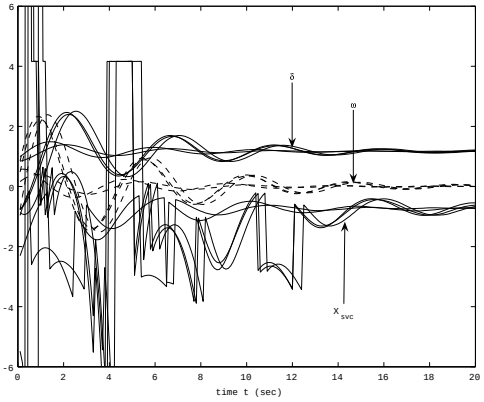

(c) PA SVC with $\lambda_{1,2} = -0.2 \pm 1.3853j$

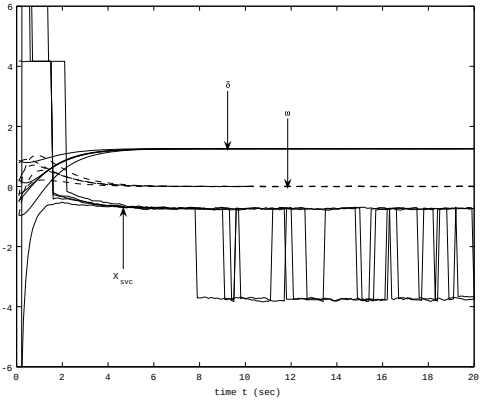

(d) PA SVC with $\lambda_1 = -0.9115$, $\lambda_2 = -2$

Figure 5: Time responses of the closed-loop IGS under PA SVCs

SVCs can also reduce overshots in the power angle curves.

(iii). Illustrative examples with PA and LQR SVCs subject to constraints.

In Figure 7, the susceptance constraints on the SVCs is $|X_{\rm SVC}| \leq 5$ (or equivalently $X_{\rm min} = -5$ and $X_{\rm max} = 5$), the closed-loop poles are allocated to $\lambda_{1,2} = -0.5 \pm 1.2542j$ so that the steady-state power angle is $\delta_e = 72°$, which is exactly what we see from all the cases of Figure 7. In each case of Figure 7, the susceptance constraints on the resulting SVCs are met but at the price that some transient features of the time responses deteriorate more or less. For example, comparing the case (a) of Figure 6 with that in (d) of Figure 7, in which the LQR SVCs are implemented for the same power angle $\delta_e = 72°$, we can see that the transient period in the latter case is generally longer than that of the former one.

It must be stressed that another price one must pay for employing SVCs subject to susceptance constraints is that bang-bang actions in SVCs are involved during the transient period. Fortunately, such swithing actions in SVCs mean no serious problems if we notice that high-frequency switchings in SVCs can be realized electrically through thyristors, instead of mechanically.

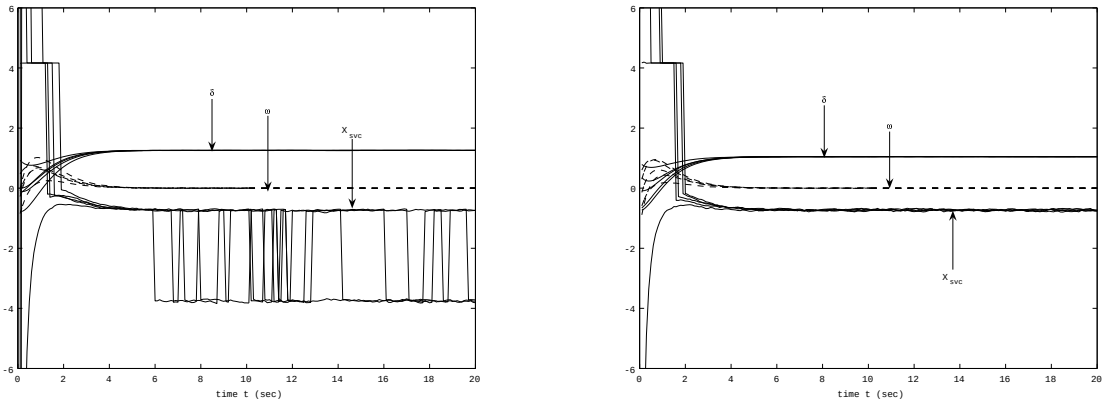

(a) LQR SVC with $\delta_e = 72°$ (b) LQR SVC with $\delta_e = 60°$

Figure 6: Time responses of the closed-loop IGS under LQR SVCs

5 Conclusions

In this paper, robust stabilization of individual generators in multimachine networks by using state feedback controlled static VAR compensators, which are designed by means of pole assignment and least quadratic regulation techniques together with the piecewise control theory [17, 32], is considered. The stabilization technique is developed through a piecewise linearization approximation of swing equations. Different from the conventional swing equations [19],[21],[22], the piecewisely linearized swing equations have LTI structural features, to which the well-developed LTI analysis and synthesis techniques apply better and conveniently. This makes it possible to accommodate other control performances as well, though in this paper only the power angle specification is examined. Last but not least, the SVC stabilization approach can be implemented to multiple generators of multimachine networks in a decentralized fashion based only on local feedback without any essential modification on the stabilization algorithms, by taking advantage of the power disturbance generator model. This is a promising advantage of the stabilization technique.

References

[1] R. Gupta, B. Bandyopadhyay and A. M. Kulkarni, Power system stabilizer for multimachine power system using robust decentralised periodic output feedback, *IEE Proceedings of Control Theory and Applications*, vol. 152, no. 1, pp. 3–8, 2005.

[2] L. F. C. Alberto and N. G. Bretas, Synchronism versus stability in power systems, *International Journal of Electrical Power & Energy Systems*, vol 21, no. 4, pp. 261–267, 1999.

[3] T. C. Yang, N. Munro and A. Brameller, A new decentralized stabilization method with application to power system stabilizer design for multimachine systems. *International Journal of Electrical Power & Energy Systems*, vol. 9, pp. 206–261, 1987.

[4] L. Cong, Y. Wang and D. J. Hill, Co-ordinated control design of genertor excitation and SVC for transient stability and voltage regulation enhancement of multi-machine power systems, *International Journal of Robust and Nonlinear Control*, vol. 14, pp. 789–805, 2004.

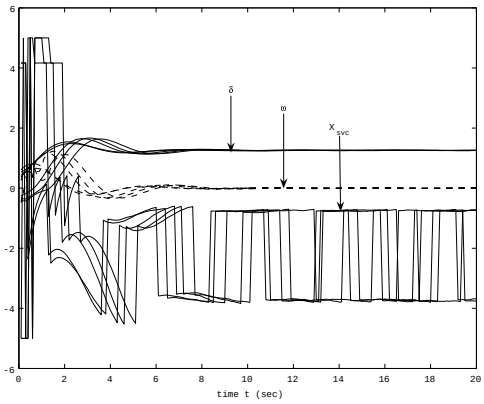

(a) PA SVC with $\lambda_{1,2} = -0.5 \pm 1.2542j$

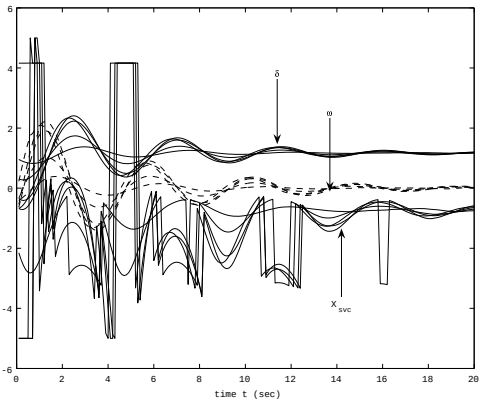

(b) PA SVC with $\lambda_{1,2} = -0.2 \pm 1.3852j$

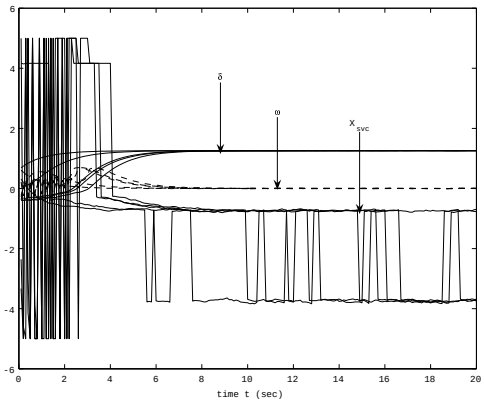

(c) PA SVC with $\lambda_1 = -0.9115$ and $\lambda_2 = -2$

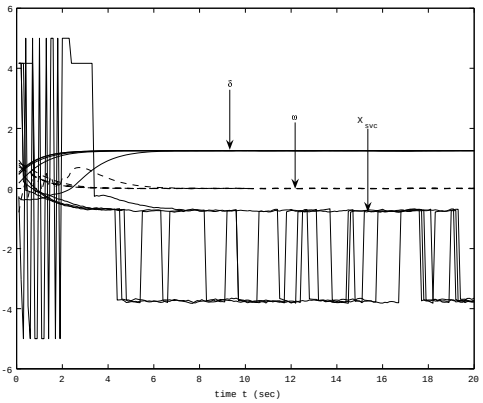

(d) LQR SVC with gain constraints

Figure 7: Time responses of the closed-loop IGS with constrainted SVCs

[5] G. Damm, R. Marino and F. Lamnabhi-Lagarrigue, Adaptive nonlinear output feedback for transient stabilization and voltage regulation ofpower generators with unknown parameters, *International Journal of Robust and Nonlinear Control*, vol. 14, pp. 833-855, 2004.

[6] Q. Lu, S. W. Mei, W. Hu, F. F. Wu, Y. X. Ni and T. L. Shen, Nonlinear decentralized disturbance attenuation excitation control via new recursive design for multi-machine power systems, *IEEE Transactions on Power Systems*, vol. 16, no. 4, pp. 729–736, 2001.

[7] L. L. Fan and A. Feliachi, Decentralized stabilization of nonlinear electric power systems using local measurements and feedback linearization, *Proceedings of the 43rd IEEE Mideast Symposium on Circuits and systems*, vol. 2. pp. 638–641, 2000.

[8] M. E. Aboul-Ela, A. A. Sallam, J. D. McCalley and A. A. Fouad, Damping controller design for power system oscillations using global signals, *IEEE Transactions on Power Systems*, vol. 11, no. 2, pp. 767–773, 1996.

[9] Y. Y. Wang, D. J. Hill, and G. X. Guo, Robust decentralized control for multimachine power systems, *IEEE Transactions on Circuits and Systems–I*, vol. 45, no. 3, pp. 271–279, 1998.

[10] M. H. Haque, Application of energy function to assess the first-swing stability of a power system with an SVC, *IEE Proc.-Gener. Transm. Distrib.,* vol. 152, no. 6, pp. 806–812, 2005.

[11] M. H. Haque, Improvement of first swing stability limit by utilizing full benefit of shunt FACTS devices, *IEEE Transactions on Power Systems*, vol. 19, no. 4. pp. 1894–1902, 2004.

[12] E. Lerch, D. Povh and L. Xu, Advanced SVC control for damping power system oscillations, *IEEE Transactions on Power Systems*, vol. 60, no. 2, pp. 524–531, 1991.

[13] A. Isidori, *Nonlinear Control Systems II*, Springer, London, 1999.

[14] T. C. Yang, Synchronous generator stabilizer design through incomplete state feedback, *International Journal of Electrical Power & Energy Systems*, vol 16, no. 2, pp. 91–95, 1994.

[15] E. Z. Zhou, Application of static VAR compensators to increase power system damping, *IEEE Transactions on Power Systems*, vol. 8, no. 2, pp. 655–661, 1993.

[16] V. I. Vorotnikov, *Partial Stabiltiy and Control*, Birkhauser, Boston, 1998.

[17] M. Johansson, *Piecewise Linear Control Systems*, Springer-Verlag, Berlin, 2003.

[18] P. M. Anderson and A. A. Fouad, *Power System Control and Stability*, 2nd Ed, Wiley-Interscience, New York, 2003.

[19] E. W. Kimbark, *Power System Stability*, Vol. I, Wiley-Interscience, New York, 1995.

[20] D. O′Regan, *Existence Theory for Nonlinear Ordinary Differential Equations*, Kluwer Academic Publishers, Dordrecht, 1997.

[21] K. R. Padiyar, *Power System Dynamics*, John Wiley & Sons Ltd, Singapore, 1996.

[22] M. Pavella and P. G. Murthy, *Transient Stability of Power Systems-Theory and Practice*, John Wiley & Sons, Chichester, 1994.

[23] M. Parashar, J. S. Thorp and C. E. Seyler, Continuum modeling of electromechanical dynamics in large-scale power sysetms, *IEEE Transactions on Circuits and Systems I*, vol. 51, no. 9, pp. 1848–1858, 2004.

[24] H. D. Chiang and C. C. Chu, Stability regions of nonlinear autonomous dynamical systems, *IEEE Transactions on Automatic Control*, vol. 33, no. 1, pp. 16–17, 1988.

[25] C. W. Liu, J. S. Thorp, J. Lu, R. J. Thomas and H. D. Chiang, Detection of transiently chaotic swings in power-systems using real-time phasor measurements, *IEEE Transactions on Power Systems*, vol. 9, no. 3, pp. 1285–1292, 1994.

[26] F. M. A. Salam, Asymptotic stability and estimating the region of attraction for the swing equations, *Systems & Control Letters*, vol. 7, no. 4, pp. 309–312, 1986.

[27] J. Machowski, J. W. Bialek and J. R. Bumby, *Power system dynamics and stability*, John Wiley & Sons, New York, 1997.

[28] M. Vidyasagar, *Nonlinear Systems Analysis*, 2nd ed., Prentice-Hall, Inc., Englewood Cliffs, NJ, 2002.

[29] J. Zhou and Y. Ohsawa, Improved swing equation and its properties in synchoronous generators, *IEEE Transactions on Circuits and Systems–I: Regular Papers*, vol. 56, no. 1, pp. 200-209, 2009. DOI: 10.1109/TCSI.2008.924895.

[30] K. Zhou and J. C. Doyle, *Essentials of Robust Control*, Prentice Hall, New York, 1998.

[31] Y. Fukusima, *Introduction to Mathematical Programming*, Asakura Bookhouse, Tokyo, 2004 (in Japanese). Prentice Hall, 1998.

[32] N. B. O. L. Pettit, *Analysis of Piecewise Linear Dynamical Systems*, John Wiley & Sons Inc., New York, 1995.